Soft-x-ray-emission studies of bulk Fe₃Si, FeSi, and FeSi₂, and implanted iron silicides

J. J. Jia, T. A. Callcott, W. L. O'Brien, and Q. Y. Dong
University of Tennessee, Knoxville, Tennessee 37996

D. R. Mueller and D. L. Ederer
National Institute of Standards and Technology, Gaithersburg, Maryland 20899

Z. Tan and J. I. Budnick
University of Connecticut, Storrs, Connecticut 06269
(Received 27 April 1992)

Bulk iron silicides and implanted iron silicides have been studied by soft-x-ray emission (SXE) spectroscopy. The Si $L_{2,3}$ emission spectra of these materials are measured. For bulk silicides, these spectra provide a measure of s- and d-type partial density of states (PDOS) localized on the Si sites. We compare them with available band-structure calculations and also with photoemission measurements. For implanted systems, the Si $L_{2,3}$ emission spectra provide useful information about the silicide formation process with the variation of implant doses.

I. INTRODUCTION

In a great number of studies[1-4] conducted on the transition-metal (TM) silicides and metal-silicon interfaces, iron silicides have received far less attention than cobalt and nickel silicides. Only a small number of electronic structure studies have been performed on iron silicides. Partly, this is due to the lower technological potential of iron silicides at present compared with either Co or Ni silicides, and partly it is due to the complex crystal structure of these materials. Yet iron silicides have very interesting electronic and magnetic properties. A more comprehensive understanding of their electronic structures certainly will help to explore these properties.

One of the three pure phase bulk Fe silicides, FeSi₂ is a good semiconductor[5] and shows potential use in combining silicon-based digital technology with new optoelectronic devices.[6] Another, Fe₃Si, has drawn considerable interest due to the site occupation preference of substitutional transition-metal impurities in this material. But it has been studied mostly by nuclear magnetic resonance (NMR) and neutron scattering techniques.[7] The magnetic properties and structural stability of the third, FeSi, are also very interesting. A clear picture of its electronic structure and chemical bonding is needed to fully understand these properties. However, our knowledge of these materials is still incomplete as far as the electronic structure and chemical bonding are concerned. We have made soft-x-ray-emission (SXE) measurements on these materials in order to gain more experimental information on the filled bands of these compounds. SXE spectroscopy is a proven method in investigating the bulk electronic structures of solid materials. Our previous studies[8,9] have demonstrated the usefulness of SXE spectroscopy in studying bulk silicides and implanted silicides. In particular, the s- and d-like partial density of states of the valence electrons localized on Si sites can be effectively studied by this method.

In this paper, we will present the Si $L_{2,3}$ emission spectra of these bulk Fe silicides and also of some iron-implanted silicon samples. In SXE spectroscopy, energetic electrons or photons are used to generate vacancies in the core levels of atoms within the specimen. Soft x rays are emitted as valence electrons radiatively recombine with the core-level vacancies. The energy distribution of these photons are detected and analyzed, which provides information about the filled valence or conduction bands of the materials studied. Because the spectra are generated in radiative transitions to a localized core hole, the spectroscopy is chemically selective and provides a local density of states (LDOS) for each element of a complex solid. In addition, the radiative transitions obey the dipole selection rule for angular momentum so that SXE spectra formally represent angular-momentum-selected partial density of states (PDOS). Also, for most operating conditions, both excitation and escape distances are sufficiently great so that SXE spectroscopy is a bulk probe which is relatively insensitive to surface conditions.

By measuring the Si $L_{2,3}$ emission spectra of iron silicides, the local s and d LPDOS's for the Si sites can be effectively probed by this method. This information is not available from photoemission measurements due to the dominance of the Fe d electrons in photoemission spectra. We will discuss the involvement of silicon s electrons in bonding and compare our results with available calculations and photoemission results. General agreement is found between our spectrum on FeSi₂ and theoretical calculations as well as previous experimental results. Some comparisons can also be made with less detailed calculations available for Fe₃Si. No detailed band-structure calculations with projected LPDOS exist in the literature for FeSi. However, some clear trends can be identified in going from iron-poor to iron-rich com-

pounds that give information about the evolution of bonding in these materials.

II. EXPERIMENT

The bulk FeSi and $FeSi_2$ samples were prepared by compressing commercially obtained powders into pellets. The powders have crystallites visibly large enough to represent the bulk properties. The Fe_3Si sample is a single crystal prepared by arc melting. Its composition and crystal structure were checked by x-ray scattering. The iron-implanted samples were prepared by uniformly implanting polished silicon (100) wafers. A scanning beam of 150-keV Fe^+ ions was used for implantation with substrate temperature maintained at about 350 °C in a vacuum of 10^{-6} Torr. The sample holder was surrounded by a liquid-nitrogen trap and warmed by a heater with temperatures monitored and stabilized during the implantation. The samples we studied here have implantation doses of 5×10^{17}, 7×10^{17}, and 1×10^{18} Fe/cm².

SXE measurements were carried out on our high-efficiency SXE spectrometer installed at the National Synchrotron Light Source, Brookhaven National Laboratory. Spectrometer and detector have been described elsewhere.[10,11] Our measurements were conducted with a 600-lines/mm grating and a 100-μm input slit. Instrumental resolution is estimated to be better than 0.2 eV at a photon energy of 100 eV. Measurements were made in an UHV chamber at a pressure of 5×10^{-9} Torr. Emission was excited by a 100-μA, 3-keV electron beam focused to a 1-mm² spot. The samples were placed on a holder located 3 or 4 mm away from the entrance slit of the spectrometer. Electrons were incident on the sample at an angle of 30° from the sample normal, and the takeoff angle for x-rays was 50°. The spectra were corrected for the nonuniform detector response and astigmatic deformation in the nondispersion direction. Complete spectra were assembled from segments taken at successive positions along the Rowland circle. Each segment covers roughly 15 Å in the silicon L emission range. Bremsstrahlung background induced in electron excitation is fitted as a straight line and subtracted from the spectra. For the 3-keV electron excitation, we estimate the penetration depth to be about 1000 Å for pure Si and to be reduced to about 300 Å for the most Fe-rich samples.

Self-adsorption effects sometimes seriously distort SXE spectra. In these studies, self-absorption effects are believed to be small and are not corrected. We confirmed this assumption by varying both the excitation energy of exciting electrons and the takeoff angle of emitted x rays, and observing that no significant changes were found in the measured spectral features.

II. RESULTS AND DISCUSSION

A. The Si $L_{2,3}$ emission of bulk Fe silicides

Figure 1 shows the Si $L_{2,3}$ emission spectra from Fe_3Si, FeSi, and $FeSi_2$. In most Si compounds these spectra can be divided into two regions. There is a peak region at
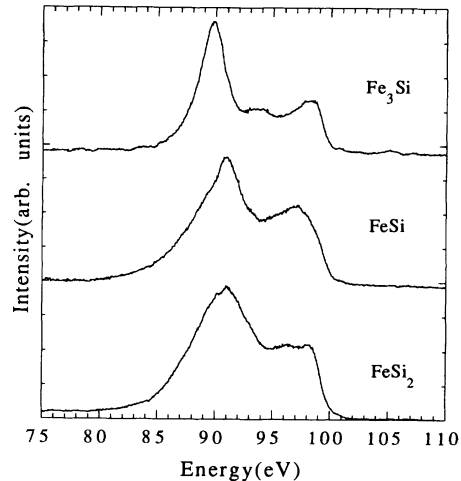

FIG. 1. The Si $L_{2,3}$ emission spectra of Fe_3Si, FeSi, and $FeSi_2$.

lower photon energies near 90 eV associated with non-bonding Si $3s$ orbitals and a shoulder region above this peak extending up to the top of the filled valence states at about 100 eV. In the peak region, the spectrum for Fe_3Si has a narrow and symmetric peak centered just below 90 eV. The major peak of the spectrum for the FeSi is asymmetric with its maximum at roughly 91 eV and a shoulder superimposed on its low-energy flank. The major feature of the spectrum for $FeSi_2$ is a nearly symmetric peak with its top flattened. The centroid of this peak is at 91 eV and it is wider than the analagous peaks from FeSi and Fe_3Si. In the shoulder region, Fe_3Si has a wide peak near the Fermi level with its maximum at approximately 98 eV and another small hump located at roughly 94 eV. The shoulder region for FeSi is a broad hump between 93.5 and 100 eV, which peaks at 97 eV. For $FeSi_2$, the shoulder is a rather flat one with two small features on top of it. One of the features is at 96.4 eV and another one is at 98 eV.

It is clear that the s-orbital peak narrows in going from Si-rich silicide to Fe-rich silicides. As we mentioned earlier, these Si s states are not involved in the bonding with the metal atoms. The width of this peak is essentially determined by the wave-function overlap of the neighboring silicon atoms. In metal-rich silicides, the Si-Si interatomic distances are increased due to the introduction of large numbers of metal atoms and the lowering of the Si concentration, which reduce the wave-function overlap between different silicon atoms.[12] The broadening is most dramatic between Fe_3Si, which has no Si nearest neighbors (Si-Si distance=3.999 Å, Ref. 7) and $FeSi_2$, which has an average Si-Si distance of 2.708 Å.[13] The detailed shape of this major feature, however, is related to the long-range order in the crystals. We recall that in elemental silicon the major feature has a very different appearance depending on whether it is crystalline or amorphous. In crystalline silicon, the s-orbital peak is splitted. In amorphous Si, the splitting is removed by filling in the region between the twin c-Si peaks, but the

overall width of the feature is essentially unchanged.[9] The basic tetrahedral local symmetry and the nearest-neighbor distances are the same in these two materials so that the width remains the same, while the long-range order in the crystalline phase splits the peak. The asymmetric shape of the major feature in the spectrum for FeSi is probably due to the irregular number and distances of Si neighbors as a result of complex cubic $B20$ crystal structure of FeSi.[14]

The broad peak centered at 98 eV, about 2 eV below the Fermi edge in the shoulder region of Fe_3Si, can be identified as the overlap of Fe d orbitals onto the Si sites, consistent with observations in our previous study on Co and Ni silicides.[8] A band-structure calculation by Switendick[15] gives the Fe d LPDOS for the two inequivalent Fe sites in this structure. In the unit cell of Fe_3Si, there are 8 Fe A,C sites at 2.449 Å from each Si and 6 Fe B sites at 2.828 Å from each Si.[7] From a comparison with this calculation, we conclude that the peak in our spectrum at 98 eV derives mostly from the A,C site LPDOS which peaks 2 eV below the Fermi edge. The B site LPDOS makes no contribution at this energy, but peaks 2 eV deeper in the band. The photoemission study by Egert and Panzner[16] also yields a broad Fe d feature close to the Fermi level.

The weak hump observed at approximately 94 eV is either due to the Si s and p hybridization or due to the Si s and Fe d bonding formation. Switendick's calculation has Si p states at this particular energy. Though transitions from p states will not contribute to our spectra, we do pick up intensity from s-p hybridizations. Thus we tentatively identify this feature with Si s-p hybridized states. We remind the reader that sp^3 hybridization is responsible for all of the intensity seen in the shoulder region in pure Si samples.

The broad feature centered at 97 eV in the shoulder region of the spectrum for FeSi is difficult to interpret at the present time. There is no detailed band-structure calculation with projected LPDOS's available for this compound. Hence our analysis is limited. Some extra intensity near the Fermi edge in the shoulder region for FeSi probably results from the d overlap from the Fe atoms surrounding the silicon sites. Photoemission measurements of FeSi (Refs. 16–18) locate the maximum of the d band very close to the Fermi level (-1 eV), so that it is unlikely that the intensity peaking 3 eV below the edge results primarily from Fe d overlap. A recent cluster calculation[19] on FeSi found that the strongest bond between Fe and Si is the Si sp-Fe sp orbital interactions (if this is true here, it is probably also true for CoSi, since it has the same crystal structure as FeSi). The same calculation also points out that although Fe d orbitals contribute to bonding significantly, they do so through electrostatic diatomic interactions. This suggests to us that the majority of the intensity of the hump centered at 97 eV in our spectrum is probably due to the Si sp hybridized states. However, the validity of cluster calculation on complex crystals such as FeSi remains questionable.

The spectrum of $FeSi_2$ can be satisfactorily explained with Christensen's calculation.[20] The experimental s and d DOS's localized on Si sites can be obtained by dividing the Si $L_{2,3}$ emission spectrum by the cube of the photon energy. The result is shown in Fig. 2 for $FeSi_2$. The binding energy of the Si $2p_{3/2}$ level was chosen at 99.8 eV, the crystalline Si $2p_{3/2}$ level binding energy. In Fig. 3 we reproduce Christensen's projected s, p, and d LPDOS's for Si and d LPDOS for Fe for atoms in one of the two inequivalent sites available to each element. The LPDOS's for atoms in the second Si and Fe sites have almost the same characteristic structures with the first and are not shown here. The Si s LPDOS in Fig. 3(a) clearly supports the flattening of the top of the major peak of our experimental spectrum. Also from Figs. 3(a) and 3(b), we notice that the Si s LPDOS extends up to the valence-band maximum and that the Si p LPDOS extends all the way down to the bottom of the valence band. So the Si s and p LPDOS's overlap completely in the region of the occupied bands. The situation is very similar to that of elemental silicon and of Co and Ni disilicides. In all these materials, the s states in the shoulder region can be associated with the sp^3 hybridization. The sp^3 hybridization is the prototype of the covalent bonding for tetrahedral symmetry. The local tetrahedral symmetry is sustained in going from elemental silicon to Co and Ni disilicides which have the CaF_2 structure. Our spectrum and Christensen's calculation show that this kind of sp^3 hybridization is still largely preserved in $FeSi_2$. This is justified by the fact that the stable structure of $FeSi_2$ deviates only slightly from the fluorite structure.

From Figs. 3(c) and 3(d), it can be seen that the Si d and Fe d LPDOS's of $FeSi_2$ peak immediately below the valence-band maximum at almost the same position. Their structures are also very similar. This probably is the origin of the peak we observed at 98 eV (-1.8 eV in Fig. 2) right below the band maximum. It is also in good agreement with the photoemission measurement of Egert and Panzner,[14] which locates the Fe d band maximum at approximately 2 eV below the Fermi level. This situation is again very similar to that of the Co and Ni disilicides where we observed features corresponding to Si d and Co (or Ni) d contributions.[8] We concluded that the involvement of Si d orbitals was due to the overlap of metal d orbitals onto the Si sites. Here again we observed that the same overlap is causing an observable feature in the Si
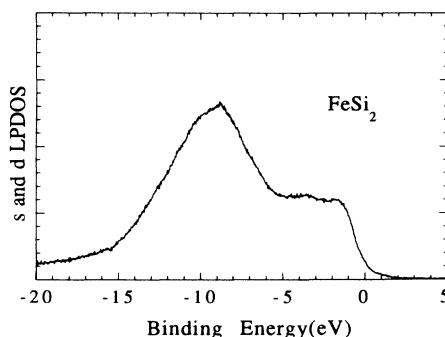

FIG. 2. The experimental s and d LPDOS's of $FeSi_2$ derived from the Si $L_{2,3}$ emission spectrum.

$L_{2,3}$ emission spectrum of FeSi$_2$.

In a similar way, the small peak at 96.4 eV (-3.4 eV) in the spectrum of FeSi$_2$ matches a shoulder in the calculated s-LPDOS [Fig. 3(a)] that coincides in energy with the major peak in the Si p-LPDOS [Fig. 3(b)], giving evidence for the persistence of s-p bonding in this material.
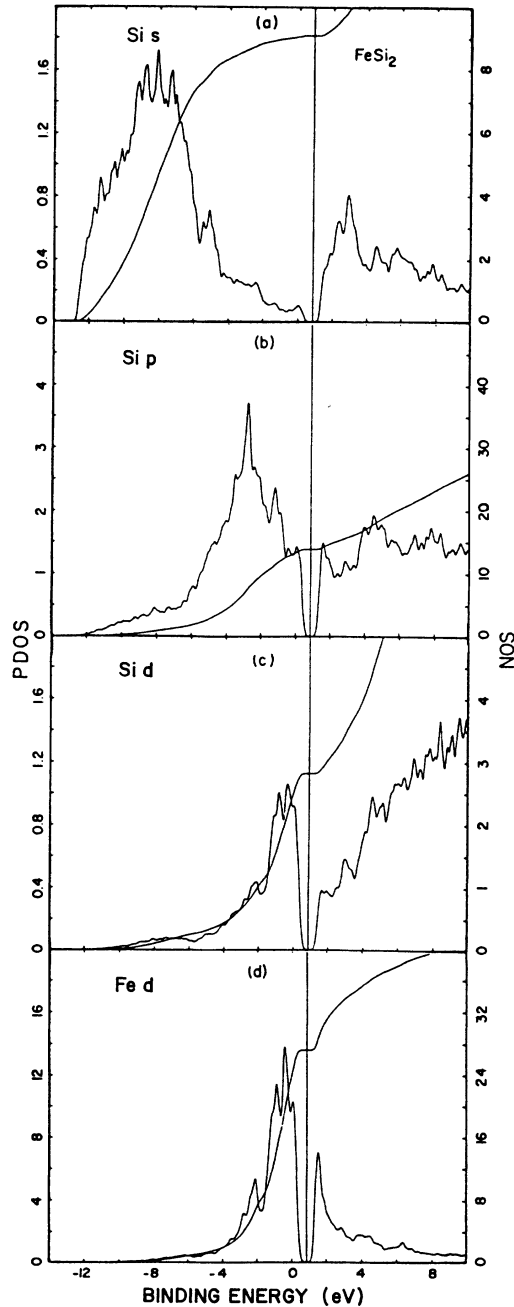
B. The Si $L_{2,3}$ emission of implanted silicon samples

Figure 4 shows the Si $L_{2,3}$ emission spectra of the implanted samples. The spectra for the implanted samples also have the familiar two regions normally observed in Si spectra of the bulk silicides discussed in the previous section: the peak at lower photon energies associated with the nonbonding Si s orbitals, and the shoulder region above this peak extending up to about 100 eV. Both of these regions change quite dramatically with increasing implantation dose, as shown in Fig. 4. In the 5×10^{17} Fe/cm^2 sample, the major peak is a broad symmetric feature with its center of gravity located between 90 and 91 eV. In the 7×10^{17} Fe/cm^2 sample, this feature appears to be slightly narrower. It also has added weight on its low-energy flank which moves its center of gravity to a lower photon energy. In the sample with the highest dose, the 1×10^{18} Fe/cm^2 sample, this peak becomes narrower and more symmetric with a center of gravity at roughly 90 eV.

The shoulder region also goes through interesting changes with increasing implantation dose. In the 5×10^{17} Fe/cm^2 sample, the spectrum closely matches that of FeSi$_2$. It exhibits two small peaks in this region that nearly match those observed in FeSi$_2$, although the one at 98 eV is a little more prominent in the implanted sample. In the 7×10^{17} Fe/cm^2 sample, the spectrum resembles that of FeSi. It has a peak at 97 eV, similar to that observed in the bulk FeSi. It also has some extra intensity between 97 and 99 eV, so the spectrum decreases rather suddenly from 98 eV, while in the bulk FeSi the spectrum decreases more gradually from 97 eV. For the 1×10^{18} Fe/cm^2 sample, there is a low intensity, broad peak at around 97 eV superimposed on a flat shoulder at this region of the spectrum.

The remarkable resemblance of the spectrum of the 5×10^{17} Fe/cm^2 sample to that of the bulk Fe disilicide

FIG. 3. The projected LPDOS's and number of states (NOS) for FeSi$_2$ by Christensen (private communication). (a) Si(1) s, (b) Si(1) p, (c) Si(1) d, and (d) Fe(1) d. The LPDOS's on the other kind of sites are very similar. The units here are (electrons/eV)/cell and (electrons/cell), respectively.
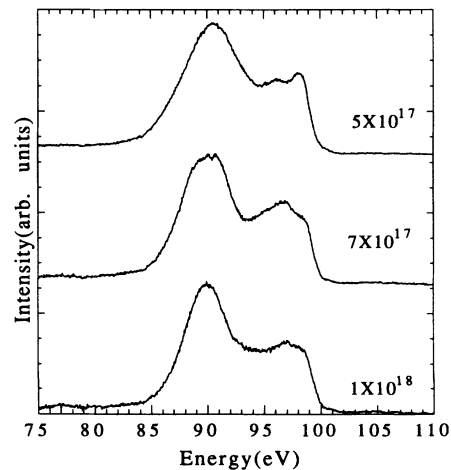

FIG. 4. The Si $L_{2,3}$ emission spectra of implanted silicon samples. The number in the graph indicates the implant dose in units of ions/cm^2.

indicates that the majority silicide phase is $FeSi_2$. This is similar to the cobalt-implanted systems where the $CoSi_2$ phase forms at a very low implantation dose $(1 \times 10^{17}$ $Co/cm^2)$ and persists at a very high implantation dose to preserve the local tetrahedral symmetry of the Si lattice.[9] Even though the β-phase $FeSi_2$ is slightly distorted from the tetrahedral symmetry in the fluorite structure, the disilicide phase is still the dominant phase at intermediate dosage $(5 \times 10^{17} Fe/cm^2)$. It is probably similar to the cobalt-implanted systems at the low doses, although we did not study them in the Fe case.

In the $7 \times 10^{17} Fe/cm^2$ sample, the existence of the monosilicide FeSi is unambiguously identified by the presence of the peak at 97 eV, which is a characteristic feature of the FeSi spectrum. The center of gravity of the major peak for this sample moves to lower photon energies and the peak gets narrower relative to the 5×10^{17} Fe/cm^2 sample, which indicates there may be a new silicide phase that comes into existence at this dosage, possibly a metal-rich one. This sample may also still contain some of the $FeSi_2$ phase, since the extra intensities at around 98 eV can only be accounted for by the presence of $FeSi_2$.

The characteristic feature of the FeSi spectrum, namely the peak at 97 eV, persists in the spectrum for the $1 \times 10^{18} Fe/cm^2$ sample. However, it is of less intensity than for the $7 \times 10^{17} Fe/cm^2$ sample. This suggests that some FeSi still exists in this high dose sample, but it occupies a smaller percentage of the volume than in the $7 \times 10^{17} Fe/cm^2$ sample. The major emission peak now is even narrower and its center of gravity is at 90 eV. We recall that none of the major peaks in the spectra of FeSi and $FeSi_2$ has its center of gravity at 90 eV. Figure 1 shows that only the spectrum of bulk Fe_3Si has its center of gravity at around 90 eV. This shows that either Fe_3Si or another metal-rich silicide phase exist in this particular sample. X-ray-diffraction (XRD) studies show that the presence of Fe_5Si_3 is also possible in this sample.[21] We did not study the $L_{2,3}$ emission of Fe_5Si_3, but we believe that its low-energy peak should be similar to Fe_3Si. Although the major peak in the spectrum for the 1×10^{18} Fe/cm^2 sample is much narrower than that in the other two implanted samples, it is still wider than that in the spectrum of the pure Fe_3Si. We conclude that this sample is probably composed of mixed phases of FeSi and Fe_3Si (or possibly Fe_5Si_3). The width of the major peak in the Si $L_{2,3}$ emission spectra is dependent on the overlap of the neighboring silicon atoms. In metal-rich silicides, the Si-Si distances are increased due to the introduction of large number of metal atoms, which reduce the wavefunction overlap between different silicon atoms.

The monosilicide and metal-rich silicides seem to form more easily in iron-implanted systems than they do in the cobalt-implanted systems, although it appears that both systems start with the disilicide phase. This could be due to the fact that it is difficult to break tetrahedral bonding in the Co disilicide. In the case of Fe, the $FeSi_2$ is already somewhat distorted from the tetrahedral symmetry. Thus it is probably easier to add more metal atoms to the disilicide core to form the monosilicide in the iron-implanted systems. Although CoSi and FeSi have the same crystal structure, it is clear that the formation of CoSi is more difficult than that of FeSi in the implantation situation.

IV. SUMMARY

We have studied three bulk iron silicides $(Fe_3Si, FeSi,$ and $FeSi_2)$ and some iron-implanted silicide systems with soft-x-ray-emission spectroscopy. We found in going from $FeSi_2$ to Fe_3Si with increased metal concentration that the Si s band becomes narrower and more isolated from the other valence states. The spectrum of $FeSi_2$ compares favorably with calculation and photoemission results. We found that the covalent bonding signature of sp^3 hybridization is still somewhat preserved in this compound. The presence of a d-like feature just below the Fermi edge in the spectrum of $FeSi_2$, and the similarity of this compound to $CoSi_2$ and $NiSi_2$, suggests the presence of Si s metal d bonding. For FeSi and Fe_3Si the narrowing of the s-orbital peak is consistent with increasing Si-Si distances. Nevertheless, there is some evidence that the Si s states still participate in bonding. Peaks associated with s-p bonding have been tentatively identified at 97 eV in FeSi and at 94 eV in Fe_3Si, and features probably related to s-d bonding appear just below the Fermi edge in both spectra. Due to the lack of theoretical input, our understanding of these two materials is necessarily incomplete. For iron-implanted silicide systems, we found that the disilicides form easily at intermediate dosage while the metal-rich phases come into existence with the increase of dose, in contrast to our previous study on cobalt-implanted systems where the disilicide phase persists even at very high doses to preserve the tetrahedral geometry.

ACKNOWLEDGMENTS

[1]L. Brillson, Surf. Sci. Rep. **2**, 123 (1982).

[2]G. W. Rubloff, Surf. Sci. **132**, 268 (1983).

[3]C. Calandra, O. Bisi, and G. Ottaviani, Surf. Sci. Rep. **4**, 271 (1984).

[4]G. Rossi, Surf. Sci. Rep. **7**, 1 (1987).

[5]U. Birkholz and J. Schelm, Phys. Status Solidi **27**, 413 (1968).

[6]N. Cherief, R. Cinti, M. de Crescenzi, J. Derrien, T. A. Nguyen Tan, and J. Y. Veuillen, Appl. Surf. Sci. **41/42**, 241 (1989).

[7]V. A. Niculescu, T. J. Burch, and J. I. Budnick, J. Magn. Magn. Mater. **39**, 223 (1983).

[8]J. J. Jia, T. A. Callcott, W. L. O'Brien, Q. Y. Dong, J.-E. Rubensson, D. L. Mueller, D. L. Ederer, Phys. Rev. B **43**, 4863 (1991).

[9]J. J. Jia, T. A. Callcott, W. L. O'Brien, Q. Y. Dong, D. L. Mueller, J.-E. Rubensson, D. L. Ederer, Z. Tan, F. Namavar, and J. I. Budnick, J. Appl. Phys. **69**, 7800 (1991).

[10]T. A. Callcott, C. H. Zhang, K. L. Tsang, E. T. Arakawa, and D. L. Ederer, Rev. Sci. Instrum. **57**, 2680 (1986).

[11]T. A. Callcott, C. H. Zhang, K. L. Tsang, D. L. Ederer, and E. T. Arakawa, Nucl. Instrum. Methods. A **266**, 578 (1988).

[12]B. Aronsson, T. Lundstrom, and S. Runqvist, *Borides, Silicides and Phosphides* (Wiley, New York, 1965).

[13]Y. Dusausoy, J. Protas, R. Wandji, and B. Roques, Acta Crystallogr. Sec. B **27**, 1209 (1971).

[14]L. Pauling and A. M. Soldate, Acta. Crystallogr. **1**, 212 (1948). (1948).

[15]A. C. Switendick, Solid State Commun. **19**, 511 (1976).

[16]B. Egert and G. Panzner, Phys. Rev. B **29**, 2091 (1984).

[17]S. J. Oh, J. W. Allen, and J. M. Lawrence, Phys. Rev. B **35**, 2267 (1987).

[18]A. Kakizaki, H. Sugawara, I. Nagakura, Y. Ishikawa, T. Komatsubara, and T. Ishii, J. Phys. Soc. Jpn. **51**, 2597 (1982).

[19]L. J. Rodriquez, F. Ruette, G. R. Castro, E. V. Ludena, and A. J. Hernandez, Theor. Chim. Acta. **77**, 39 (1990).

[20]N. E. Christensen, Phys. Rev. B **42**, 7148 (1990).

[21]Z. Tan, F. Namavar, J. I. Budnick, F. H. Sanchez, A. Fasihuddin, S. M. Heald, C. E. Bouldin, and J. C. Woicik (unpublished).